Dynamic magnetism in the disordered hexagonal double perovskite $BaTi_{1/2}Mn_{1/2}O_3$

M. R. Cantarino,[1] R. P. Amaral,[2] R. S. Freitas,[1] J. C. R. Araújo,[2] R. Lora-Serrano,[2] H. Luetkens,[3] C. Baines,[3] S. Bräuninger,[4] V. Grinenko,[4] R. Sarkar,[4] H. H. Klauss,[4] E. C. Andrade,[5] and F. A. Garcia[1]

[1]*IFUSP, Universidade de São Paulo, 05508-090 São Paulo-SP, Brazil*

[2]*Universidade Federal de Uberlândia, Instituto de Física, 38400-902 Uberlândia-MG, Brazil*

[3]*Laboratory for Muon Spin Spectroscopy, Paul Scherrer Institute, CH-5232 Villigen PSI, Switzerland*

[4]*Institute for Solid State and Material Physics, TU Dresden, D-01069 Dresden, Germany*

[5]*Instituto de Física de São Carlos, Universidade de São Paulo, C.P. 369, São Carlos, 13560-970 São Paulo-SP, Brazil*

(Received 7 March 2018; revised manuscript received 31 January 2019; published 15 February 2019)

Magnetic frustration and disorder are key ingredients to prevent the onset of magnetic order. In the disordered hexagonal double perovskite $BaTi_{1/2}Mn_{1/2}O_3$, Mn^{4+} cations, with $S = 3/2$ spins, can either form highly correlated states of magnetic trimers or dimers or remain as weakly interacting orphan spins. At low temperature (T), the dimer response is negligible, and magnetism is dominated by the trimers and orphans. To explore the role of magnetic frustration, disorder and possibly of quantum fluctuations, the low-T magnetic properties of the remaining magnetic degrees of freedom of $BaTi_{1/2}Mn_{1/2}O_3$ are investigated. Heat-capacity data and magnetic susceptibility display no evidence for a phase transition to a magnetically ordered phase but indicate the formation of a correlated spin state. The low-temperature spin dynamics of this state is then explored by μSR experiments. The zero-field μ^+ relaxation rate data show no static magnetism down to $T = 19$ mK and longitudinal field experiments support as well that dynamic magnetism persists at low T. Our results are interpreted in terms of a spin-glass state which stems from a disordered lattice of orphans spins and trimers. A spin liquid state in $BaTi_{1/2}Mn_{1/2}O_3$, however, is not excluded and is also discussed.

DOI: 10.1103/PhysRevB.99.054412

I. INTRODUCTION

Transition-metal (M) oxides are forever the source of intriguing physics in the field of correlated electron systems, including a large number of complex magnetic systems [1]. Complexity emerges from the magnetic interaction between the spins at the M sites, which takes place by means of a superexchange interaction [2] that will usually drive the system to a magnetic ordered state [3]. In some materials, however, dimensionality, disorder, lattice geometry, or the symmetry of the interactions may hinder the appearance of long-range order [4–8]. In these cases, the system will remain in a dynamic magnetic state. This dynamic magnetic state may either be identified as a spin freezing phenomenon [9,10] or, at sufficient low temperatures (T), the system may be driven by quantum fluctuations to some exotic ground state, such as a quantum spin liquid ground state. A spin liquid state is a disordered quantum magnetic state wherein the spins are entangled in a highly correlated and dynamic state of matter [11–13].

The first task to experimentally verify the formation of a spin liquid state is to provide evidence for the lack of phase transitions down to the lowest temperatures. It is paramount, as well, to present evidence that a collective spin state is formed at low T, most striking by characterizing continuous magnetic excitations [14–16] or the spin-relaxation rate regime. For the latter purpose, muon spin relaxation (μSR) is a particular appropriate technique [17–20]. The task, however, cannot be settled based upon μSR measurements alone, since a dynamic magnetic state without strong quantum fluctuations (such as a spin glass) will also display an evolution of the relaxation regime [9,21] which holds some similarity to what is found for some spin liquid candidates [20,22].

In the disordered hexagonal double perovskite $BaTi_{1/2}Mn_{1/2}O_3$, $S = 3/2$ spins due to Mn^{4+}cations pair up to form magnetic dimers in a singlet state, coexisting with orphan spins and magnetic trimers [23]. The formation of dimers and trimers is dictated by large energy scales ($\approx$101–176 K). The effective low-T degrees of freedom involve orphan spins and trimers, distributed in layers of triangular lattices, with competing antiferromagnetic exchange interactions. The distinct layers are well spaced, making the interactions mainly of intralayer character. As we shall discuss, this distribution of orphans and trimers implies a large magnetic frustration, with a lower bound for the frustration parameter (f) of about $\sim$75.

In this paper, we show that this configuration paves the way for the existence of a dynamic magnetic state at low T in our system, comprised of correlated $S = 3/2$ (orphans) and effective $S = 1/2$ spins (trimers). We present and discuss low -T heat capacity and susceptibility data which show no sign of long-range order, but which indicate a highly correlated magnetic state. Subsequently, we explore the spin dynamics of our system by μSR, and it is shown that dynamic magnetism persists down to the lowest temperatures ($T = 0.019$ K) achieved in our experiments. Our results and analysis support that this dynamic magnetic state can be interpreted as a spin-glass state. However, a spin liquid scenario is not excluded and is discussed as well.

II. METHODS

High quality polycrystalline samples were synthesized by the solid-state reaction method as in Ref. [23]. Synchrotron x-ray-diffraction experiments were carried out at the XRD1 beamline of the LNLS-CNPEM, Brazil [24]. Heat-capacity measurements were performed for temperatures down to 0.1 K and magnetic fields up to 9 T, employing a Quantum Design PPMS, using a dilution refrigerator. dc and ac susceptibility [$\chi(T)$ and $\chi'(T)$] measurements were performed for temperatures down to 0.6 K employing a Quantum Design MPMS (1.8–300 K) and a vibrating sample magnetometer (VSM) in a ^{3}He cryostat.

μSR measurements have been carried out at the πM3 beam line at the GPS and LTF spectrometers of the Swiss Muon Source at the Paul Scherrer Institute (PSI) in Villigen. The measurements were performed in the T interval $0.019 < T < 10$ K (LTF) and $1.5 < T < 200$ K (GPS) [25] in zero magnetic field (ZF) and in longitudinal applied magnetic fields (LF) with respect to the initial muon spin polarization up to 0.05 T. To improve the thermal contact, the samples in the experiments at the LTF spectrometer were glued on a Ag plate. This gives rise to a time- and temperature-independent background due to muons that stopped in the Ag plate. The μSR time spectra were analyzed using the free software package MUSRFIT [26]. DFT calculations of the electrostatic potential were performed to extract information about the muon local environment. We employed the all-electron full-potential linearized augmented plane-wave code Elk 4.3.6, which includes the Spacegroup package using Broyden mixing [27] and the generalized gradient approximation functional [28].

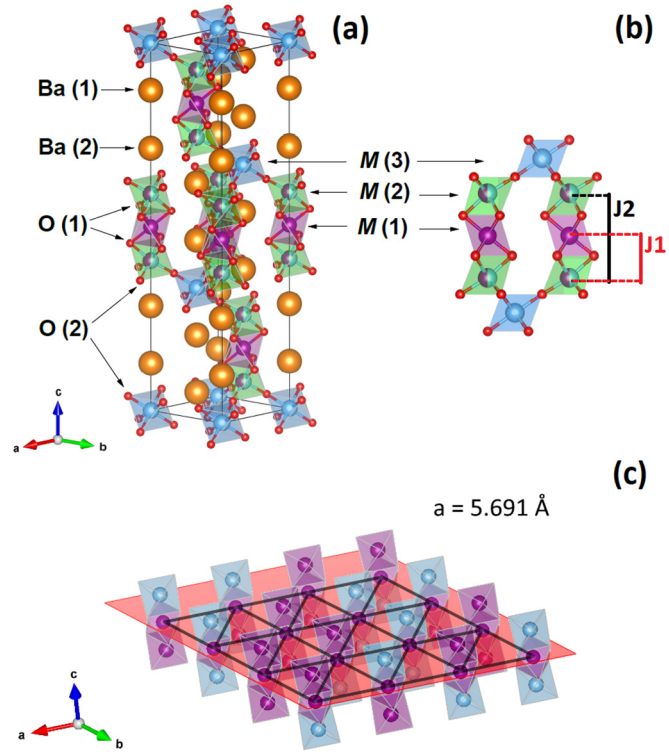

FIG. 1. (a) Structural model of $BaTi_{1/2}Mn_{1/2}O_3$ with a 12R-type perovskite structure (as in Ref. [23]). Barium [Ba(1) and Ba(2)], oxygen [O(1) and O(2)], and transition metal [$M(1)$, $M(2)$ and $M(3)$] sites are indicated. (b) Detail of the structural trimer indicating the J_1 and J_2 exchange constants. (c) Model of the proposed emerging magnetic lattice at low T. Half of the $M(2)$ sites are filled with Mn atoms (purple) and the other half by Ti atoms (blue), in a disordered way, that is statistically determined.

III. RESULTS AND DISCUSSION

A. Structure, magnetism, and heat capacity

The $BaTi_{1/2}Mn_{1/2}O_3$ structure is presented in Fig. 1(a) [23,29,30] (see Ref. [31] for further support from new resonant diffraction experiments). The structure possesses three transition metal sites, termed $M(1)$, $M(2)$, and $M(3)$. Mn cations are found at the $M(1)$ and $M(2)$ sites, inside the structural trimers. The $M(1)$ sites are occupied exclusively by Mn atoms whereas the occupation of the $M(2)$ sites is mixed.

All analyses so far [23,29,30] and our results [31] support that the $M(2)$ site is equally occupied by either Mn or Ti atoms. Therefore, the relative fractions of dimers, trimers, and orphans are statistically determined as in Ref. [23]. It results that 1/8 of the Mn are orphans, half pair up to form dimers, and 3/8 form trimers. The coupling of magnetic dimers and trimers are described by two strong exchange constants J_1 and J_2 [Fig. 1(b)], which were shown to be of comparable size [23].

As a function of T, the dimer contribution to magnetism is exponentially suppressed and we can safely assume that at low T the remaining magnetic degrees of freedom are due to orphan spins and magnetic trimers. Focusing on the plane formed by the $M(1)$ sites, one may propose the following emerging two-dimensional (2D) structure for the magnetic lattice, represented in Fig. 1(c): layers of randomly distributed magnetic trimers and orphans and dimers in a triangular lattice (lattice constant $a = 5.69$ Å). The dimers, being nonmagnetic at low T, act essentially to dilute the magnetic interactions in the system. Distinct layers of this magnetic lattice are in a AB stacking and interlayer interaction may be possible, however, consecutive layers are separated by ≈ 9.8 Å and this interaction is likely weak.

In Fig. 2(a) we present heat-capacity measurements C_p as a function of T ($0.2 < T < 100$ K) for distinct values of H. The data give no evidence for a phase transition down to $T = 0.2$ K, presenting only a broad anomaly peaking at about 3 K for $H = 0$, that we shall interpret as a crossover to the dynamic magnetic state. Below and about $T \lesssim 0.2$ K, the data present an upturn at low T that could be interpreted as the tail of a transition at further lower temperatures. This upturn, however, is actually due to the Mn nuclear contribution to the heat capacity. This conclusion is supported by the data presented in the inset of the same figure, wherein we compare the $H = 0$ data with the Mn nuclear heat capacity as measured in experiments with MnNi [32]. It is shown that it scales well with our data and, therefore, it is safe to assert that no phase transition is observed down to $T \approx 0.1$ K.

In panel (b), $\chi(T)$ measurements are presented in the interval $0.6 < T < 330$ K. To describe the data in the range $T > 5.5$ K, which is above the crossover region, we refer

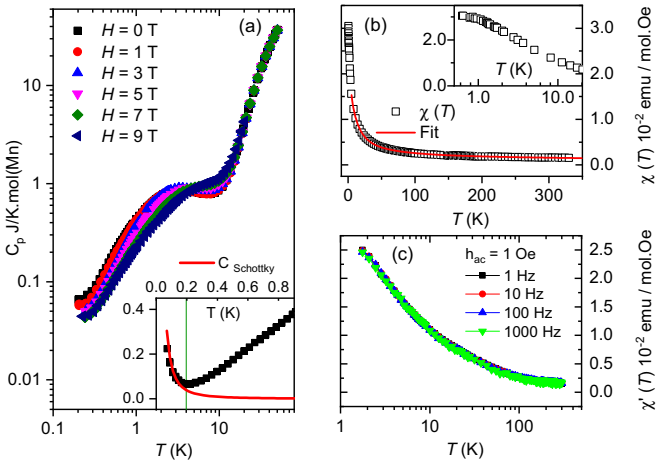

FIG. 2. (a) Heat-capacity (C_p) measurements as a function of T and applied field H. The inset shows the Mn nuclear contribution to the heat capacity. (b) dc susceptibility [$\chi(T)$] measurements as a function of T ($0.6 \leqslant T \leqslant 330$ K). The inset shows $\chi(T)$ data for $T < 2$ K. The fitting (thick line) is discussed in Ref. [31]. (c) ac susceptibility [$\chi'(T)$] measurements as a function of T ($1.8 \leqslant T \leqslant 300$ K) at distinct frequencies.

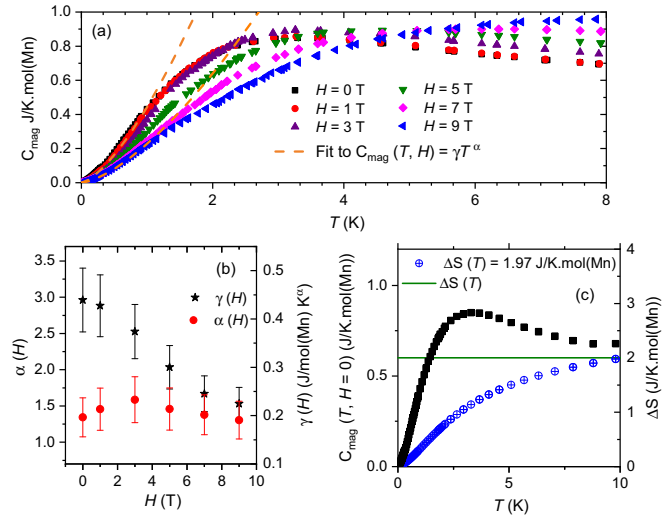

FIG. 3. (a) Magnetic specific heat, $C_{\rm mag}(T)$, obtained after the subtraction of the lattice contribution. The dashed lines are representative fittings ($H = 0$ and $H = 9$ T) to $C_{\rm mag}(T) = \gamma(H)T^{\alpha(H)}$. (b) Full set of field dependent parameters $\gamma(H)$ and $\alpha(H)$ obtained from this fitting. (c) Zero-field magnetic specific-heat data and the total magnetic entropy $\Delta S(T)$.

to our model [31] including magnetic dimers and trimers plus orphan spins. The obtained parameters associated to dimers and trimers are $J_1 = 176(5)$ K and $J_2 = 0.59(5)J_1$. In this parameter range, the trimer ground state is formed by effective $S = 1/2$ spins, which, along with the $S = 3/2$ spins from the Mn^{4+} orphans, are the remaining magnetic degrees of freedom at low T. In the inset can be observed a trend towards saturation which cannot be related to a simple Curie-Weiss behavior. It rather indicates the absence of free paramagnetic spins in the system and thus we conclude that the effective $S = 1/2$ spins and orphan spins are correlated at low T.

To estimate the energy scale of the correlated state of trimers and orphans, we model the orphan-trimer subsystem by a Curie-Weiss susceptibility, with parameters $\theta_{\rm eff}$ and $C_{\rm eff}$, obtaining $\theta_{\rm eff} = -7.5(5)$ K and $C_{\rm eff} = 0.19(1)$ emu K/mol (f.u.) [31]. The value of $\theta_{\rm eff}$ supports the idea of a highly frustrated system, with a lower bound for the frustration parameter of $f \gtrsim 7.5/0.1 = 75$. Here, $\theta_{\rm eff}$ is to be understood as a phenomenological constant which sets the energy scale of the interactions between the remaining magnetic degrees of freedom: orphan-orphan, orphan-trimer, and trimer-trimer interactions. In the context of the discussion of Fig. 1(c), it reflects mainly the intralayer interactions of the diluted magnetic lattice. As for $C_{\rm eff} = 0.19(1)$ emu K/mol (f.u.), it compares relatively well with $C \approx 0.14$ emu K/mol (f.u.) expected for 1/16 mols of Mn $S = 3/2$ plus effective $S = 1/2$ spins per formula unit of $BaTi_{1/2}Mn_{1/2}O_3$. In Fig. 2(c), $\chi'(T)$ measurements ($1.8 < T < 300$ K) at a broad range of frequencies (ν) do not depend on ν even in the interval 1.8–3 K, that is below the crossover region. Such dependency could be expected, for instance, in spin-glass systems.

The nature of the dynamic magnetic state will manifest in the behavior of magnetic specific heat $C_{\rm mag}$. Following the subtraction of the phonon contribution ($C_{\rm lattice}$, [31]), $C_{\rm mag}$ is presented in Fig. 3(a) for H up to 9 T. Inspecting the broad anomalies, we observe that the peaks displace to higher temperatures (from $T \approx 3$–7 K) with increasing field. To characterize the magnetic excitations of the low-T phase, we focus on the low-temperature region ($0.2 \leqslant T \leqslant 1.0$ K). It is adopted that $C_{\rm mag}(T)$ will in general follow a power law in the low -T region and the data are fitted to the expression $C_{\rm mag}(T) = \gamma(H)T^{\alpha(H)}$. The dashed lines are representative ($H = 0$ T and $H = 9$ T) fittings. The resulting parameters, $\gamma(H)$ and $\alpha(H)$, are shown in Fig. 3(b). Within error bars, $\alpha(H)$ is nearly constant assuming a value of about $\approx$1.45(5), suggesting gapless excitations of this low-T dynamic magnetic phase. Moreover, $C_{\rm mag}/T$ do not diverge as $T \to 0$, meaning that our system is away from quantum criticality [33]. The value of $\gamma(H)$ decreases with increasing field from $\gamma \approx 0.45$ to $\gamma \approx 0.25$ J/mol(Mn) K^{α} at $H = 9$ T, indicating quenching of the magnetic entropy as a function of the field, albeit there are no free spins in the system at this temperature range. These values are relatively large when compared to spin liquid candidates [34].

The nature of the zero field $C_{\rm mag}$, in particular, is key to estimate the total entropy recovered in the ground state and to reveal the total fraction of spins that are part of the proposed correlated state. In Fig. 3(c), we show the heat-capacity data and the magnetic entropy [$\Delta S(T)$] for $H = 0$ in the interval $0.1 \leqslant T \leqslant 10$ K, within which the entropy contribution from excited states of the trimer is negligible. The total entropy recovered by the system amounts to $\approx$1.97(5) J/K mol (Mn). This number must be compared with the entropy expected from the remaining magnetic degrees of freedom at low T [31], that amounts to 1/8 mol of $S = 3/2$ and effective $S = 1/2$ spins per mol of Mn atoms. Thus, the total expected entropy is $R/8(\ln 4 + \ln 2) \approx 2.16$ J/K mol (Mn). The experimental result is certainly larger than what is

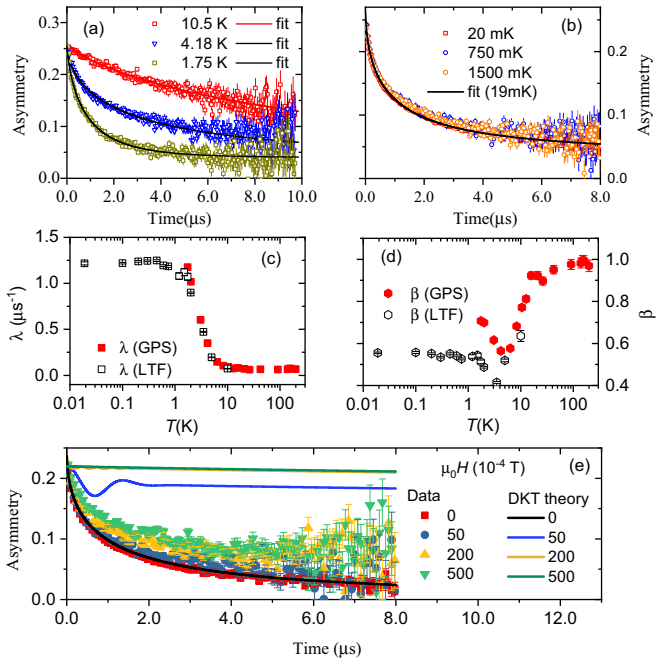

FIG. 4. (a),(b) Representative ZF-μSR spectra measured at the (a) crossover region and (b) in the low-T region. Thick lines are the fittings of the data to a stretched exponential. Temperature dependency of the (c) μ^+ spin-relaxation rate, λ and (d) stretching exponent β as a function of T. (e) LF experiment ($T = 0.1$ K) spectra and comparison with the DKT theory.

expected for the orphan spins only [$\approx$1.44 J/K mol (Mn)], further suggesting that the remaining magnetic degrees of freedom must include $S = 3/2$ and effective $S = 1/2$ spins. Moreover, the trimers cannot be in a simple paramagnetic state for such state would imply (i) sizable Schottky anomalies in the field dependent heat-capacity measurements, and (ii) a Curie-like response in the magnetic susceptibility, both which are not observed [31]. Overall, if we consider the total entropy due to trimers and orphans in the system, we may assert that we recover a total of $\approx$90% of the expected system entropy.

B. μSR ZF and LF experiments

We now turn our attention to our μSR experiments [18]. In Figs. 4(a)–4(d) we present ZF μSR data measured for temperatures down to $T = 0.019$ K. Down to the lowest temperatures, the spectra [Figs. 4(a)–4(b)] can be described quite well by an exponential decay, and the data do not present the characteristic damped oscillations of a magnetic ordered phase [18]. Figure 4(a) shows the temperature interval for which the spectra change the most ($1.5 < T < 10$ K), characterizing a crossover behavior in this region. Figure 4(b) displays the low-temperature spectra, which can be almost described by a single fitting below $T < 1.5$ K. The theoretical curves represent the best fitting to a stretched exponential which describes the asymmetry function $A(t) = A_0 \exp -(\lambda t)^{\beta} + B$, where A_0 is the starting asymmetry, B describes the constant background mostly due to muons that did not stop in the sample, and λ and β are, respectively, the relaxation rate and the stretching exponent. The muon environment was investigated by means of DFT calculations. The result proposes that the muon is located close to the oxygen between the two barium sites [31].

The resulting fitting parameters λ and β are shown in Figs. 4(c) and 4(d). For $T > 10$ K, λ is nearly temperature independent, as typical for simple paramagnets. In the T region $1.5 < T < 10$ K, λ goes through a steep increase from $\approx 0.06\ \mu s^{-1}$ up to a constant value $\approx 1.2\ \mu s^{-1}$ for $T < 1.5$ K, characteristic of a crossover behavior. The β coefficient also displays a crossover behavior in this same T region. Its value decreases from $\approx$1 at high T to a constant value close to 0.5 for $T < 1.5$ K. This value is well above 1/3 that would be expected for glassy dynamics of simple systems, indicating the absence of static local fields [9,18]. It is noteworthy that the crossover region detected by the μSR corresponds closely to the region where the broad peak is observed for the heat-capacity measurements. Our data illustrate a good qualitative agreement between macroscopic and microscopic measurements.

We have as well performed LF measurements at $T = 0.1$ K and the results are presented in Fig. 4(e). The data are compared with the expected results from the dynamical Kubo-Toyabe (DKT) theory. The change in the spectra as a function of field (from 0 to 0.05 T) is much less dramatic than the expected from the DKT theory. This is a compelling piece of evidence for dynamic magnetism at temperatures down to $T = 0.1$ K. Following Refs. [17,19], the spin fluctuation rates for temperatures above and below the crossover can be estimated [31]. The results are $\nu_{T>10\,\mathrm{K}} = 7.4(1) \times 10^{10}$ Hz and $\nu_{T<1.5\,\mathrm{K}} = 3.7(6) \times 10^{6}$ Hz, suggesting, without symmetry breaking, the onset of long-time spin correlations in the system for $T < 1.5$ K.

C. Nature of the dynamic magnetic state

By direct inspection, the ZF spectra at low T in Fig. 4(b) lack the characteristic recovery of 1/3 of the μ^+ polarization expected for glassy systems [9], thus we start discussing the possibility of a spin liquid state. The experimental results from heat capacity are compatible with a gapless spin liquid. Because the magnetic susceptibility saturates at low T, a strong candidate would be a spin liquid with a spinon Fermi surface. However, for the latter, we expect $C_{\mathrm{mag}} \sim T^{2/3}$ [19,35] at zero field, unlike the $\approx T^{1.4\text{–}1.5}$ we observe. Another possibility would be a $U(1)$ Dirac spin liquid [36–38]. Here, one expects $C_{\mathrm{mag}} \sim T^2$ at zero fields and $C_{\mathrm{mag}} \sim T$ at low fields, and that C_{mag} should increase with the field, which we also do not observe.

A similar drawback is recently under debate in $YbMgGaO_4$, where the observed spin liquid behavior is not captured by the minimal theoretical model [15,19,34,39]. One possible scenario to understand the reported experimental behavior is to take into account the presence of disorder in the system [40], which may have nontrivial effects, even leading to the destruction of long-range magnetic order [41–43]. Since the μSR results for $YbMgGaO_4$ are qualitatively similar to ours [19], disorder is likely a relevant parameter to understand the behavior of $BaTi_{1/2}Mn_{1/2}O_3$.

In this line of thinking, the large jump in λ is a drawback to the interpretation in terms of a spin liquid state,

since it is reminiscent of spin-glass behavior [9,17,21,44]. Furthermore, a spin-glass state is favored by the presence of a disordered magnetic lattice of $S = 3/2$ and effective $S = 1/2$ spins as suggested by our structural analysis. However, large jumps of λ can be found as well for $PbCuTe_2O_6$ [20] or $Tm_3Sb_3Zn_2O_{14}$ [22], which are all recently proposed spin liquid candidates, presenting a characteristic large λ of about $\approx 1.0\ \mu s^{-1}$ at low T, as in the present case. The steep increase in λ suggests a glass transition temperature (T_g) of about $T_g \approx 1$–2 K and this must be contrasted with the frequency independence of $\chi'(T)$, especially in the region 1.8–3 K. Certainly, $\chi'(T)$ measurements down to lower temperatures are needed for a more conclusive statement.

Based upon the heat-capacity analysis, we can account for 90% of the total entropy of the system. This result almost exclude the possibility that the probed dynamic magnetic state could relate to a crossover region to an ordered state at further lower temperature. In particular, ferrimagnetic order due to the antiferromagnetic coupling of the unlike $S = 3/2$ and $S = 1/2$ spins [45,46] is not to be expected. The existence of residual entropy is compatible with a spin glass and the dynamic magnetism probed by the ZF spectra at 0.019 K could be due to the fraction of spins that are not frozen due a distribution of time scales in a spin glass. However, residual entropy is also observed in spin liquid candidates [47,48]. In short, the low-T dynamic magnetic state in our system displays spin liquid behavior, although a spin-glass state, induced by the disordered lattice of orphans and trimers [41–43], is a strong candidate to interpret our results.

IV. SUMMARY AND CONCLUSIONS

We have performed macroscopic and microscopic experiments in the disordered hexagonal double perovskite $BaTi_{1/2}Mn_{1/2}O_3$. This complex material displays a rich magnetic behavior with the physics at high temperatures dominated by the presence of trimers, dimers, and orphan spins [23]. At lower temperatures, the effective magnetic degrees of freedom, composed by orphan spins and trimers, are found to be correlated but no phase transition is detected down to $T = 0.1$ K, despite the effective exchange couplings being of the order of 10 K. μSR measurements then show substantial evidence for dynamic magnetism down to $T = 0.019$ K, the nature of which was discussed in terms of a spin liquid and a spin-glass scenario. The proper characterization of this state requires further theoretical and experimental efforts.

ACKNOWLEDGMENTS

M.R.C. acknowledges CNPq Grant No. 131117/2017-3 for financial support. The authors acknowledge CNPEM-LNLS for the concession of beam time (Proposal No. 20160245). The XRD1 beamline staff is acknowledged for the assistance during the experiments. R.S.F. acknowledges FAPESP Grant No. 2015/16191-5 and CNPq Grant No. 306614/2015-4. R.L.S. acknowledges FAPEMIG-MG (Grant No. APQ-02256-12) and CAPES Foundation (Brazil) for Grant No. EST-SENIOR-88881.119768/2016-01. V.G. was supported by DFG (GR 4667). R.S. and H.H.K. were partially supported by DFG SFB 1143 for the project C02. E.C.A. acknowledges FAPESP Grant No. 2013/00681-8 and CNPq Grant No. 302065/2016-4.

[1] E. Dagotto, Science **309**, 257 (2005).
[2] J. B. Goodenough, *Magnetism And The Chemical Bond* (Wiley, New York, 1963).
[3] R. M. White, *Quantum Theory of Magnetism Magnetic Properties of Materials* (Springer, Berlin, 2007).
[4] P. W. Anderson, Mater. Res. Bull. **8**, 153 (1973).
[5] N. Read and S. Sachdev, Phys. Rev. Lett. **62**, 1694 (1989).
[6] A. Kitaev, Ann. Phys. (January Special Issue) **321**, 2 (2006).
[7] J. S. Helton, K. Matan, M. P. Shores, E. A. Nytko, B. M. Bartlett, Y. Yoshida, Y. Takano, A. Suslov, Y. Qiu, J.-H. Chung, D. G. Nocera, and Y. S. Lee, Phys. Rev. Lett. **98**, 107204 (2007).
[8] M. Mourigal, M. Enderle, A. Klöpperpieper, J.-S. Caux, A. Stunault, and H. M. Rønnow, Nat. Phys. **9**, 435 (2013).
[9] Y. J. Uemura, T. Yamazaki, D. R. Harshman, M. Senba, and E. J. Ansaldo, Phys. Rev. B **31**, 546 (1985).
[10] R. Moessner and A. P. Ramirez, Phys. Today **59**(2), 24 (2006).
[11] L. Balents, Nature (London) **464**, 199 (2010).
[12] L. Savary and L. Balents, Rep. Prog. Phys. **80**, 016502 (2017).
[13] Y. Zhou, K. Kanoda, and T.-K. Ng, Rev. Mod. Phys. **89**, 025003 (2017).
[14] T.-H. Han, J. S. Helton, S. Chu, D. G. Nocera, J. A. Rodriguez-Rivera, C. Broholm, and Y. S. Lee, Nature (London) **492**, 406 (2012).
[15] J. A. M. Paddison, M. Daum, Z. Dun, G. Ehlers, Y. Liu, M. B. Stone, H. Zhou, and M. Mourigal, Nat. Phys. **13**, 117 (2017).
[16] C. Balz, B. Lake, J. Reuther, H. Luetkens, R. Schönemann, T. Herrmannsdörfer, Y. Singh, A. T. M. Nazmul Islam, E. M. Wheeler, J. A. Rodriguez-Rivera, T. Guidi, G. G. Simeoni, C. Baines, and H. Ryll, Nat. Phys. **12**, 942 (2016).
[17] Y. J. Uemura, A. Keren, K. Kojima, L. P. Le, G. M. Luke, W. D. Wu, Y. Ajiro, T. Asano, Y. Kuriyama, M. Mekata, H. Kikuchi, and K. Kakurai, Phys. Rev. Lett. **73**, 3306 (1994).
[18] S. J. Blundell, Contemp. Phys. **40**, 175 (1999).
[19] Y. Li, D. Adroja, P. K. Biswas, P. J. Baker, Q. Zhang, J. Liu, A. A. Tsirlin, P. Gegenwart, and Q. Zhang, Phys. Rev. Lett. **117**, 097201 (2016).
[20] P. Khuntia, F. Bert, P. Mendels, B. Koteswararao, A. V. Mahajan, M. Baenitz, F. C. Chou, C. Baines, A. Amato, and Y. Furukawa, Phys. Rev. Lett. **116**, 107203 (2016).
[21] G. T. Tran, P.-H. T. Nguyen, C. J. Bloed, M. E. Evans, J. A. Anczarski, W. P. Martin, J. Toro, D. V. Papakostas, J. Beare, M. N. Wilson, J. E. Greedan, G. M. Luke, T. Gredig, J. P. Carlo, and S. Derakhshan, Phys. Rev. B **98**, 184401 (2018).
[22] Z.-F. Ding, Y.-X. Yang, J. Zhang, C. Tan, Z.-H. Zhu, G. Chen, and L. Shu, Phys. Rev. B **98**, 174404 (2018).
[23] F. A. Garcia, U. F. Kaneko, E. Granado, J. Sichelschmidt, M. Hölzel, J. G. S. Duque, C. A. J. Nunes, R. P. Amaral, P. Marques-Ferreira, and R. Lora-Serrano, Phys. Rev. B **91**, 224416 (2015).

[24] A. M. G. Carvalho, D. H. C. Araújo, H. F. Canova, C. B. Rodella, D. H. Barrett, S. L. Cuffini, R. N. Costa, and R. S. Nunes, J. Synchrotron Radiat. **23**, 1501 (2016).
[25] A. Amato, H. Luetkens, K. Sedlak, A. Stoykov, R. Scheuermann, M. Elender, A. Raselli, and D. Graf, Rev. Sci. Instrum. **88**, 093301 (2017).
[26] A. Suter and B. M. Wojek, Phys. Procedia **30**, 69 (2012).
[27] G. P. Srivastava, J. Phys. A: Math. Gen. **17**, L317 (1984).
[28] J. P. Perdew, K. Burke, and M. Ernzerhof, Phys. Rev. Lett. **77**, 3865 (1996).
[29] G. M. Keith, C. A. Kirk, K. Sarma, N. M. Alford, E. J. Cussen, M. J. Rosseinsky, and D. C. Sinclair, Chem. Mater. **16**, 2007 (2004).
[30] L. Miranda, A. Feteira, D. C. Sinclair, K. Boulahya, M. Hernando, J. Ramirez, A. Varela, J. M. Gonzalez-Calbet, and M. Parras, Chem. Mater. **21**, 1731 (2009).
[31] See Supplemental Material at http://link.aps.org/supplemental/10.1103/PhysRevB.99.054412 for details of the data treatment, complementary data, and some explanatory notes.
[32] W. Proctor, R. G. Scurlock, and E. M. Wray, Proc. Phys. Soc. **90**, 697 (1967).
[33] Y. Singh, Y. Tokiwa, J. Dong, and P. Gegenwart, Phys. Rev. B **88**, 220413 (2013).
[34] Y. Li, H. Liao, Z. Zhang, S. Li, F. Jin, L. Ling, L. Zhang, Y. Zou, L. Pi, Z. Yang, J. Wang, Z. Wu, and Q. Zhang, Sci. Rep. **5**, 16419 (2015).
[35] O. I. Motrunich, Phys. Rev. B **72**, 045105 (2005).
[36] Y. Ran, M. Hermele, P. A. Lee, and X.-G. Wen, Phys. Rev. Lett. **98**, 117205 (2007).
[37] S. Ryu, O. I. Motrunich, J. Alicea, and M. P. A. Fisher, Phys. Rev. B **75**, 184406 (2007).
[38] Y.-C. He, M. P. Zaletel, M. Oshikawa, and F. Pollmann, Phys. Rev. X **7**, 031020 (2017).
[39] Y. Li, G. Chen, W. Tong, L. Pi, J. Liu, Z. Yang, X. Wang, and Q. Zhang, Phys. Rev. Lett. **115**, 167203 (2015).
[40] Y. Li, D. Adroja, R. I. Bewley, D. Voneshen, A. A. Tsirlin, P. Gegenwart, and Q. Zhang, Phys. Rev. Lett. **118**, 107202 (2017).
[41] Z. Zhu, P. A. Maksimov, S. R. White, and A. L. Chernyshev, Phys. Rev. Lett. **119**, 157201 (2017).
[42] E. C. Andrade, J. A. Hoyos, S. Rachel, and M. Vojta, Phys. Rev. Lett. **120**, 097204 (2018).
[43] E. Parker and L. Balents, Phys. Rev. B **97**, 184413 (2018).
[44] A. Keren, P. Mendels, I. A. Campbell, and J. Lord, Phys. Rev. Lett. **77**, 1386 (1996).
[45] E. Lieb and D. Mattis, J. Math. Phys. **3**, 749 (1962).
[46] Y. Iqbal, T. Müller, P. Ghosh, M. J. P. Gingras, H. O. Jeschke, S. Rachel, J. Reuther, and R. Thomale, Phys. Rev. X **9**, 011005 (2019).
[47] R. Kumar, D. Sheptyakov, P. Khuntia, K. Rolfs, P. G. Freeman, H. M. Rønnow, T. Dey, M. Baenitz, and A. V. Mahajan, Phys. Rev. B **94**, 174410 (2016).
[48] R. Kumar, P. Khuntia, D. Sheptyakov, P. G. Freeman, H. M. Rønnow, B. Koteswararao, M. Baenitz, M. Jeong, and A. V. Mahajan, Phys. Rev. B **92**, 180411 (2015).